

## The low-temperature magnetism of cerium atoms in $\text{CeMn}_2\text{Si}_2$ and $\text{CeMn}_2\text{Ge}_2$ compounds

This article has been downloaded from IOPscience. Please scroll down to see the full text article.

2004 J. Phys.: Condens. Matter 16 6685

(<http://iopscience.iop.org/0953-8984/16/37/005>)

View [the table of contents for this issue](#), or go to the [journal homepage](#) for more

Download details:

IP Address: 129.252.86.83

The article was downloaded on 27/05/2010 at 17:32

Please note that [terms and conditions apply](#).

# The low-temperature magnetism of cerium atoms in $\text{CeMn}_2\text{Si}_2$ and $\text{CeMn}_2\text{Ge}_2$ compounds

Milan V Lalić<sup>1,3</sup>, José Mestnik-Filho<sup>2</sup>, Artur W Carbonari<sup>2</sup> and Rajendra N Saxena<sup>2</sup>

<sup>1</sup> Departamento de Física, Universidade Federal de Sergipe, Rod. Marechal Rondon s/n, 49100-000, Aracaju, Brazil

<sup>2</sup> Instituto de Pesquisas Energéticas e Nucleares, CP 11049, 05422-970 São Paulo, SP, Brazil

E-mail: mlalic@fisica.ufs.br and jmestnik@ipen.br

Received 20 May 2004, in final form 26 July 2004

Published 3 September 2004

Online at [stacks.iop.org/JPhysCM/16/6685](http://stacks.iop.org/JPhysCM/16/6685)

doi:10.1088/0953-8984/16/37/005

## Abstract

The low-temperature magnetic properties of the Ce atoms in the intermetallic compounds  $\text{CeMn}_2\text{Ge}_2$  and  $\text{CeMn}_2\text{Si}_2$  were studied. Previous neutron scattering measurements did not detect an ordered moment at Ce atoms in either compound despite the fact that they are surrounded by the Mn moments ordered ferromagnetically in the  $\text{CeMn}_2\text{Ge}_2$  and antiferromagnetically in the  $\text{CeMn}_2\text{Si}_2$ . Contrasting with this result, a recent measurement performed with the time differential perturbed angular correlation (TDPAC) technique showed the presence of a pronounced magnetic hyperfine field (MHF) at Ce sites in the  $\text{CeMn}_2\text{Ge}_2$  compound and no MHF in  $\text{CeMn}_2\text{Si}_2$ . The absence of the Ce magnetic moment and MHF in the silicide can be understood in terms of too weak a Ce–Ce magnetic interaction while in the germanide the TDPAC result suggests that some magnetic ordering of Ce atoms may occur. Aiming to understand the effects which result in the quenching of the Ce 4f moment in both cases, we performed first-principles band-structure calculations for both systems, using the full potential linear augmented plane wave method. It is shown that the magnetism of the Ce sublattice has fundamentally different nature in  $\text{CeMn}_2\text{Si}_2$  and  $\text{CeMn}_2\text{Ge}_2$ . While the Ce atoms are intrinsically non-magnetic in the silicide, having a zero magnetic moment with both spin and orbital contributions identically zero, they display magnetic properties in the  $\text{CeMn}_2\text{Ge}_2$  since their very small total moment is composed of finite spin and orbital components which almost cancel each other accidentally.

## 1. Introduction

A family of ternary intermetallic compounds  $\text{RT}_2\text{X}_2$  (where R is a rare earth, T a transition metal and X either Si or Ge) have attracted significant attention since they exhibit a rich variety

<sup>3</sup> On leave from: Institute of Nuclear Sciences ‘Vinča’, PO Box 522, 11001 Belgrade, Yugoslavia.

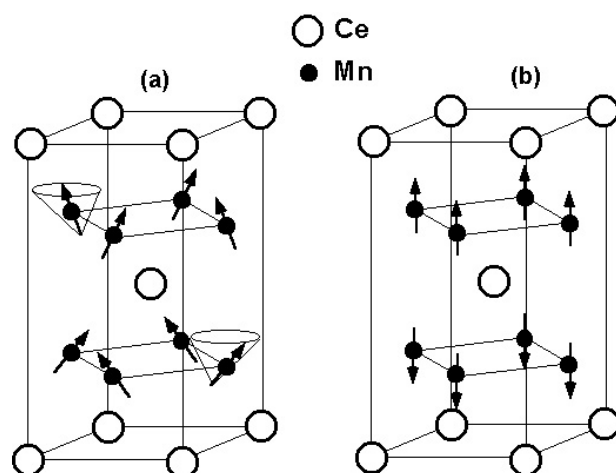


**Figure 1.** Low-temperature magnetic structures of the  $\text{CeMn}_2\text{Ge}_2$  (a) and  $\text{CeMn}_2\text{Si}_2$  (b) compounds. The non-magnetic Ge and Si atoms are not shown.

of magnetic phenomena [1, 2]. The crystal structure of these compounds is body-centred tetragonal (space group  $I4/mmm$ ), with R, T and X atoms occupying 2a, 4d and 4e positions respectively. The structure can be viewed as a repeating sequence of stacked atomic layers of the form R–X–T–X–R–... arranged perpendicularly to the tetragonal  $c$ -axis.

Among the most studied  $\text{RT}_2\text{X}_2$  compounds are those with  $T = \text{Mn}$ , owing to the fact that only in these systems do the T atoms order magnetically at high temperatures. Within this  $\text{RMn}_2\text{X}_2$  sub-family, the compounds which have attracted special attention are those with  $R = \text{Ce}$ . They are the only ones that exhibit magnetic moments exclusively at Mn sites, maintaining a quenched rare-earth 4f moment even at the lowest temperatures.

The magnetic properties of the  $\text{CeMn}_2\text{Ge}_2$  and  $\text{CeMn}_2\text{Si}_2$  have been re-examined recently by a neutron diffraction study [3]. No trace of any magnetic order at the Ce sublattices has been registered down to  $T = 12$  K, for both compounds. Neutron scattering measurements performed down to  $T = 2$  K, in the case of  $\text{CeMn}_2\text{Ge}_2$ , reached the same conclusion [4]. The magnetic structures of both the compounds at low temperatures are shown in figure 1.

In this paper we will show that the non-magnetic behaviour of Ce atoms has completely different origins in  $\text{CeMn}_2\text{Si}_2$  and  $\text{CeMn}_2\text{Ge}_2$  compounds. To arrive at this conclusion we recall the temperature dependence of magnetic hyperfine fields (MHFs) at the Ce sites in these systems, as recently measured by the time differential perturbed angular correlation (TDPAC) method [5]. Then we perform first-principles density-functional calculations for both compounds, simulating the magnetic configurations of the Mn sublattices as shown in figure 1. It is shown that in  $\text{CeMn}_2\text{Ge}_2$  the Ce atoms have a non-trivial magnetic nature since their essentially zero magnetic moment is composed of the finite spin and orbital components which almost cancel each other. In the  $\text{CeMn}_2\text{Si}_2$ , on the other hand, the Ce atoms are magnetically completely inactive, with zero magnetic moment composed of zero spin and zero orbital components.

## 2. TDPAC experimental data

Recently, our group performed an extensive experimental study of hyperfine interactions in the  $\text{CeMn}_2\text{Si}_2$  and  $\text{CeMn}_2\text{Ge}_2$  compounds, using the TDPAC technique [5]. In the present

work we will focus on a specific result of this study, namely, the temperature dependence of the Larmor frequency  $\omega_L = g\mu_N B_{\text{hf}}/\hbar$  (a quantity proportional to the MHF  $B_{\text{hf}}$ ) measured at the Ce nuclei in both compounds. The  $\omega_L$ , measured in the temperature range between 10 and 420 K, exhibits an especially interesting behaviour in the case of  $\text{CeMn}_2\text{Ge}_2$ , as shown in figure 6 of [5]. A quick look at this figure reveals that there are three temperature regimes in which the Ce MHF exhibits completely different characteristics.

- (1) Above  $T_C \approx 320$  K, in the antiferromagnetic regime, no MHF is observed. This is a consequence of symmetric arrangements of the ‘up’ and ‘down’ moments in the Mn sublattice and the weaknesses of Ce–Ce magnetic interactions.
- (2) Between  $T_C \approx 320$  K and  $T \approx 120$ –150 K, in the ferromagnetic regime, a non-zero MHF is registered. This MHF is usually referred to as transferred field, since it reflects the magnetic order of the neighbouring atoms and follows its temperature dependence in the form of a Brillouin function. Indeed, the Ce  $\omega_L$  versus  $T$  curve behaves in the same way as the  $\omega_L$  versus  $T$  curve measured at the Mn sites in  $\text{CeMn}_2\text{Ge}_2$  [6], down to  $T \approx 120$ –150 K.
- (3) Below  $T \approx 120$ –150 K the Ce MHF exhibits a deviation from the Brillouin-like behaviour. The Larmor frequency suffers a jump, having a value  $\omega_L = 2094(4)$  Mrad  $\text{s}^{-1}$  at  $T = 10$  K, which is more than twice the value of  $\omega_L = 928(2)$  Mrad  $\text{s}^{-1}$  measured at  $T = 120$  K. A steep jump of the Larmor frequency occurs at temperatures at which no magnetic or structural phase transition is reported. The  $\text{CeMn}_2\text{Ge}_2$  is in a ferromagnetic phase, the Mn moment is saturated [4] and the Larmor frequency measured at Mn positions does not exhibit any deviation from the standard Brillouin shape [6]. Therefore, all the arguments trying to explain the low-temperature jump of the Ce MHF on the basis of the Mn influence need to be discarded. It must be the Ce itself that creates an additional non-zero MHF at temperatures lower than 120–150 K, and this MHF, superposed on the transferred MHF, produces the effect as seen in figure 6 of [5].

A question that emerges is that of how the non-magnetic Ce atom can create this additional non-zero MHF. And are the Ce atoms in  $\text{CeMn}_2\text{Ge}_2$  really non-magnetic?

In the case of the  $\text{CeMn}_2\text{Si}_2$  compound, no magnetic hyperfine interaction at the Ce nuclei has been observed in the whole temperature range from 10 to 420 K [5].

### 3. First-principles calculations

The theoretical description of Ce compounds often encounters difficulties due to the controversial nature of the Ce 4f electrons. In most of the rare-earth materials the 4f states are well localized and contain an integer number of electrons. In these cases they have an atomic-like character, giving rise to a large local magnetic moments [7]. There are, however, a number of systems in which the 4f electrons behave as itinerant ones, where the 4f states should be described as ordinary Bloch states within the band theory [8–10]. Therefore, in Ce-based compounds it is not known *a priori* whether the Ce 4f states should be treated as localized or as itinerant [11]. In the case of  $\text{CeMn}_2\text{Ge}_2$  and  $\text{CeMn}_2\text{Si}_2$ , this choice was simplified owing to two facts:

- (1) it is known that the Ce MHF is about one order of magnitude smaller than the MHF of an isolated  $\text{Ce}^{3+}$  ion [12] and
- (2) the significant quenching of the  $\text{Ce}^{3+}$  free ion 4f moment ( $5/2 \mu_B$ ) is smaller than the neutron scattering detection limit [3, 4].

Both facts indicate that the Ce 4f moment is significantly quenched and then the Ce 4f states sense large crystal field effects and extensively hybridize with other states, which is a clear sign of delocalization. Consequently, we treated the Ce 4f states as band states in a valence panel, together with the Ce 5d and 6s, the Mn 3d and 4s, and the Ge (or Si) 4s and 4p (3s and 3p) states.

For band-structure calculations we used the full potential linear augmented plane wave (FP-LAPW) method [13, 14] as implemented in the WIEN2k computer code [15]. The exchange and correlation effects were treated within a generalized gradient approximation (GGA) [16]. The body-centred tetragonal unit cell has been utilized for the  $\text{CeMn}_2\text{Ge}_2$  compound. For  $\text{CeMn}_2\text{Si}_2$  this unit cell had to be doubled in order to account for an antiferromagnetic alignment of the Mn moments. For lattice parameters, as well as for internal parameters which define the positions of the Ge and Si atoms inside the unit cell, the experimental values determined at  $T = 12$  K were used [3]. They are:  $a = 4.129$  Å,  $c/a = 2.640$ ,  $z = 0.3820$  for germanide; and  $a = 3.991$  Å,  $c/a = 2.629$ ,  $z = 0.3805$  for silicide. The parameter  $R_{\text{KMAX}}$ , which controls the number of basis functions, was set to 9.0 in the  $\text{CeMn}_2\text{Ge}_2$  case and 8.0 in the  $\text{CeMn}_2\text{Si}_2$  case. In the germanide the Brillouin zone was sampled with 196  $k$ -points in its irreducible wedge, while in the silicide 135  $k$ -points have been used.

In the case of the  $\text{CeMn}_2\text{Ge}_2$  compound, the spin polarized ferromagnetic calculations were performed first. The resulting magnetic structure of the compound was found to be ferrimagnetic. The calculated Mn spin moment of  $2.33 \mu_{\text{B}}$  agrees well with the experimental value of  $2.4(2) \mu_{\text{B}}$  [3]. At the Ce atom, however, an antiparallel spin moment of  $-0.68 \mu_{\text{B}}$  was developed, in contradiction with the experimental data.

In order to induce an orbital contribution to the magnetic moment, a second spin polarized ferromagnetic calculation, but with inclusion of the spin-orbit coupling, was performed. The  $c$ -axis of the crystal was chosen as the magnetization axis. In this way the low-temperature magnetic structure of the  $\text{CeMn}_2\text{Ge}_2$  compound, as shown in figure 1, was approximated by the ferromagnetic alignment of the Mn moments along the crystalline  $c$ -axis. When compared with the previous calculations, the resulting total Mn magnetic moment was found to be practically unchanged,  $2.36 \mu_{\text{B}}$ , consisting almost completely of the 3d spin contribution. To our surprise the Ce spin moment also did not change much, having a value of  $-0.70 \mu_{\text{B}}$ . This moment originates mostly from the 4f shell ( $-0.58 \mu_{\text{B}}$ ), but with a non-negligible contribution from the 5d shell ( $-0.10 \mu_{\text{B}}$ ) as well. Additionally, a large Ce orbital moment of  $+0.54 \mu_{\text{B}}$  was developed, originating totally from the 4f shell. Being antiparallel to the spin moment, as expected from the third Hund's rule, it makes the total Ce magnetic moment  $-0.16 \mu_{\text{B}}$ , much closer to the experimental value.

The valence of the Ce ion in  $\text{CeMn}_2\text{Si}_2$  and  $\text{CeMn}_2\text{Ge}_2$  was experimentally measured and the results [17, 18] showed an instability of the Ce valence for  $\text{CeMn}_2\text{Si}_2$  with a intermediate valence of 3.12 and a stable  $\text{Ce}^{3+}$  state for  $\text{CeMn}_2\text{Ge}_2$ . The results of our calculations, which simulate the ground state of the compounds and thus are valid for  $T = 0$  K, are also in good agreement with these observations. The resulting number of 4f electrons was 0.98 in  $\text{CeMn}_2\text{Si}_2$  and 1.05 for  $\text{CeMn}_2\text{Ge}_2$ .

The main results from the calculations presented in this section are summarized in table 1.

#### 4. Discussion

The emergence of the ferrimagnetic order in  $\text{CeMn}_2\text{Ge}_2$  can be qualitatively understood on the basis of the electronic structure features of the compound. The states which dominate the  $\text{CeMn}_2\text{Ge}_2$  electronic spectrum and determine its magnetism are the Ce 4f and 5d and the Mn 3d states. Their partial densities of states (PDOS) are presented in figure 2. As expected,

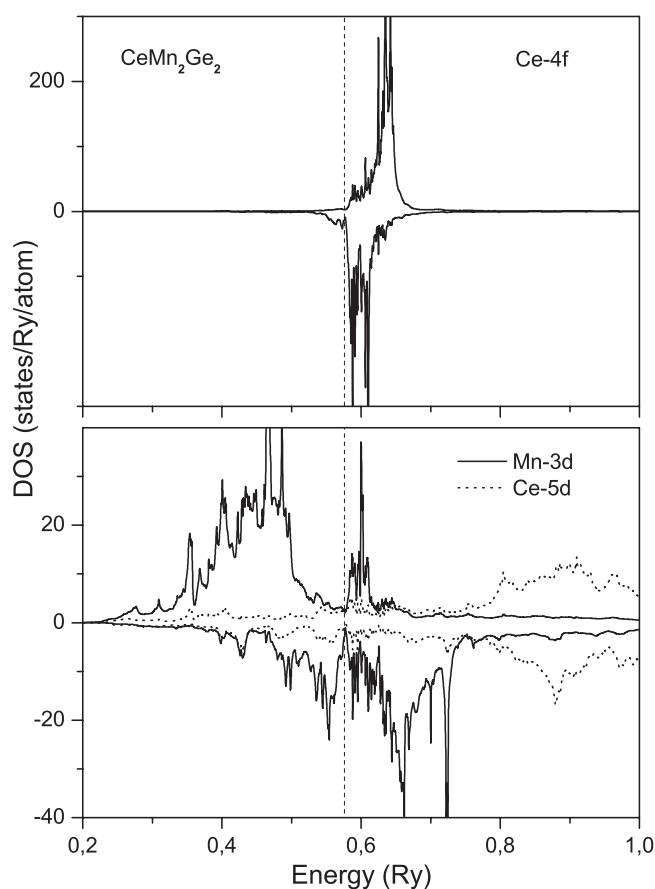


**Figure 2.** The calculated PDOS for the Ce 4f and 5d and the Mn 3d states in the  $\text{CeMn}_2\text{Ge}_2$  compound. The dashed line denotes the Fermi level.

**Table 1.** Magnetic moments, in units of  $\mu_B$ , at the Ce and Mn sites in  $\text{CeMn}_2\text{Ge}_2$  and  $\text{CeMn}_2\text{Si}_2$  compounds, as calculated by the FP-LAPW method. Experimental moments determined from the neutron scattering measurements [3] are presented for comparison.

		Spin	Orbital	Total	Neutron scattering
$\text{CeMn}_2\text{Ge}_2$	Ce	-0.70	+0.54	-0.16	0.00
	Mn	+2.35	+0.01	+2.36	2.4(2)
$\text{CeMn}_2\text{Si}_2$	Ce	0.00	0.00	0.00	0.00
	Mn	1.98	0.00	1.98	1.9(2)

the Ce 4f states are pinned at the Fermi level and form a narrow band of width of  $\sim 2.2$  eV. In a region below the Fermi energy, where the Mn 3d states are dominant, the Ce 5d PDOS strictly follows the features of the Mn 3d PDOS, a clear sign of hybridization. This 3d–5d hybridization is especially pronounced and strong for the spin down channel. It causes a charge transfer between the bands and induces the Ce 5d spin to be antiparallel to the inducing Mn 3d spin. A local ferromagnetic exchange interaction then aligns the Ce 4f spin with the

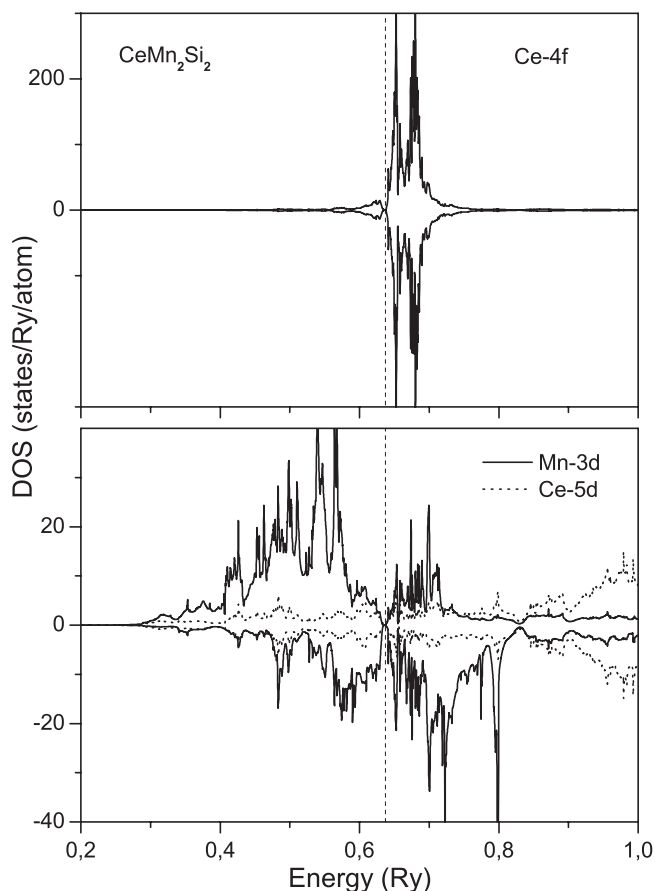


**Figure 3.** The calculated PDOS for the Ce 4f and 5d and the Mn 3d states in the  $\text{CeMn}_2\text{Si}_2$  compound. The Mn states shown belong to the Mn atom in which the spin up states are majority states. The dashed line denotes the Fermi level.

Ce 5d spin, so the total Ce spin moment is antiparallel to the Mn spin moment. Since the calculated Ce orbital moment is smaller than its spin moment, the total Ce magnetic moment stays antiparallel to the Mn magnetic moment. The mechanism just described is already used to explain the ferrimagnetic coupling between rare-earth (R) spins and transition metal (T) spins in  $\text{RT}_2$  intermetallic compounds [19].

In the case of the  $\text{CeMn}_2\text{Si}_2$  compound, the spin polarized and the spin polarized + spin-orbit calculations gave the same results: the Mn magnetic moment of  $1.98 \mu_B$ , in good agreement with the experimental value of  $1.9(2) \mu_B$  [3], and the Ce magnetic moment zero, also in agreement with the experiment [3]. The Ce zero total moment was found to be composed of zero spin and zero orbital components.

The  $\text{CeMn}_2\text{Si}_2$  electronic spectrum, presented in figure 3, shows a completely symmetric disposition of the Ce 4f and 5d spin up and spin down bands, a feature which prevents the appearance of a finite spin moment at the Ce sites. Although hybridization between the Mn 3d and the Ce 5d states is evident, the symmetric rearrangement of the neighbouring antiferromagnetic Mn moments around the Ce induces exactly the same spin up and spin down Ce 5d moments, which therefore cancel each other. Without any 5d moment and due to the

absence of the Ce–Ce interactions, the Ce 4f moment does not have a preferential direction to align with, and quenches completely.

It is a known fact that the atoms with itinerant f electrons can possess a large orbital moment [20]. Those with less than half-filled f shell have the spin and orbital moments oppositely directed (according to Hund's third rule), which allows the possibility of their partial cancellation. In such a case the atom could have a very small or eventually zero moment, but finite spin and orbital components. It could not be considered as intrinsically non-magnetic, and its compounds would form a new type of magnetic materials: ones which are neither transition metal-like nor rare-earth-like [21]. Such a situation is already encountered in the case of U atoms in some compounds (in UFe<sub>2</sub> [22] and UNi<sub>2</sub> [23] for example). Our calculations for the Ce atom magnetism in CeMn<sub>2</sub>Ge<sub>2</sub>, presented in the previous section, lead to the same situation. In both kinds of calculations (performed with and without spin–orbit coupling) a relatively large spin moment was formed on the Ce. The only way the experimental Ce moment could be reproduced was by the development of an orbital moment in the opposite direction which could partially cancel the spin moment. This scenario almost occurred as a result of the spin polarized + spin–orbit calculations (table 1). We suppose that two main factors precluded a more extensive cancellation of these moments:

- (1) the fact that we approximated the non-collinear Mn magnetic structure (figure 1) by the collinear structure of the Mn moments along the *c*-axis; and
- (2) the fact that the local density approximation (and therefore the GGA) has a tendency to underestimate the magnitude of the orbital moment [24].

It is possible that the second deficiency could have been alleviated if we went beyond the GGA and took into account the Ce 4f intra-band Coulomb correlations. In this case we could expect the splitting between occupied and unoccupied f electron states of Ce atoms. The occupied part would move towards lower energies localizing the 4f electron, in which case it should exhibit a larger moment. Since the experiment indicates a delocalized nature of the Ce 4f shell, it is expected that the effective electron correlations are not so strong. They might, however, be able to change the spin and orbital components of the Ce magnetic moment a little, and therefore lead to better quantitative agreement with the experiment.

If one accepts the theoretical indication that the Ce magnetic moment in CeMn<sub>2</sub>Ge<sub>2</sub> exhibits a strong cancellation of its non-zero spin and orbital components, the TDPAC experimental data, shown in figure 6 of [5], can be easily explained. The measured MHF results from an interaction between the nuclear magnetic dipole moment and the extra-nuclear magnetic field generated by the electronic subsystem in the crystal. It can emerge due to the spin polarized charge density of s or p<sub>1/2</sub> electrons at the nuclear position (contact field), due to the orbital magnetic moment of open electronic shells (orbital field), and due to the electronic spins (spin dipolar field). One part of the measured Ce MHF in CeMn<sub>2</sub>Ge<sub>2</sub> is the contact field, caused by the 6s shell polarization and transferred from the Mn sublattice. If the Ce atoms were intrinsically non-magnetic, this would be the only contribution to the MHF, exhibiting the Brillouin function form over the whole temperature interval. In the presence of finite spin and orbital moment in the Ce outer shells, however, the other two contributions to the MHF arise: the orbital field

$$B_{\text{orb}} = \frac{e}{mc} \langle \Phi | \frac{T(\mathbf{r}, \epsilon)}{r^3} \mathbf{L} | \Phi \rangle; \quad (1)$$

and the spin dipolar field

$$B_{\text{dip}} = \frac{e}{mc} \langle \Phi | \frac{T(\mathbf{r}, \epsilon)}{r^3} [3(\mathbf{S} \cdot \hat{\mathbf{r}})\hat{\mathbf{r}} - \mathbf{S}] | \Phi \rangle. \quad (2)$$



Both formulae were derived within the framework of the scalar relativistic approximation [25].  $T(\mathbf{r}, \epsilon) = \{1 + [\epsilon - V(\mathbf{r})]/2mc^2\}^{-1}$  is the reciprocal of the electronic relativistic mass enhancement;  $\mathbf{L}$  and  $\mathbf{S}$  are the operators of orbital and spin angular moments respectively,  $\epsilon$  is the electronic energy and  $V(\mathbf{r})$  is the crystalline potential. Averaging is performed using the large component  $|\Phi\rangle$  of the crystalline four-component wavefunction, which is an eigenspinor of the Dirac Hamiltonian without the hyperfine interaction term included.

The important information that the above formulae offer is that the eventual cancellation of the finite orbital and spin moments ( $\mathbf{L} + \mathbf{S} = 0$ ) does not necessarily lead to cancellation of their contributions to the MHF: the spatial averaging of the vector operators over the wavefunction, implicit in equation (2), significantly wipes out the spin contribution to the MHF. Since this does not occur for the orbital contribution, the MHF is much more sensitive to orbital than to spin effects. Moreover, the spin and orbital magnetization densities exhibit different spatial distributions [26] and even different temperature dependences [27]. Hence, at low temperatures, a finite Ce 4f orbital moment creates an orbital field at the Ce nucleus, which is not compensated by the corresponding spin dipolar field of the opposite sign [28].

## 5. Conclusions

In  $\text{CeMn}_2\text{Si}_2$  and  $\text{CeMn}_2\text{Ge}_2$  compounds, the measured Ce magnetic moment is known to be close to zero despite the different magnetic orders exhibited by the Mn atoms. We re-examined the nature of the Ce magnetism in these compounds by calculating their ground state properties using the FP-LAPW method, and by interpreting the temperature dependence of the MHFs measured at the Ce sites using the TDPAC technique. For  $\text{CeMn}_2\text{Ge}_2$  the MHF curve follows a Brillouin-like form at higher temperatures, reflecting the ferromagnetic order of neighbouring Mn moments. Below 120–150 K, however, the curve exhibits a deviation caused by a non-zero contribution to the MHF from the Ce sublattice. We explained this contribution via the assumption that the Ce develops finite spin and orbital magnetic moments which strongly cancel each other. The FP-LAPW calculations supported this explanation. In the case of  $\text{CeMn}_2\text{Si}_2$  the Ce MHF was found to be zero over the whole temperature range, indicating a complete magnetic inactivity of the Ce sublattice. This was confirmed by calculations which resulted in zero values for both spin and orbital components of the Ce magnetic moment.

## Acknowledgments

Partial support for this research was provided by the Fundação de Amparo à Pesquisa do Estado de São Paulo (FAPESP). MVL gratefully acknowledges the support from FAPESP in the form of a post-doctoral research fellowship.

## References

- [1] Szytula A and Leciejewicz J 1989 *Handbook on Physics and Chemistry of Rare Earths* vol 12, ed K A Gschneidner Jr and L Eyring (Amsterdam: North-Holland) p 133
- [2] Kolmakova M P, Sidorenko A A and Levitin R Z 2002 *Low Temp. Phys.* **28** 653
- [3] Fernandez-Baca J A, Hill P, Chakoumakos B C and Ali N 1996 *J. Appl. Phys.* **79** 5398
- [4] Welter R, Venturini G, Ressouche E and Malaman B 1995 *J. Alloys Compounds* **218** 204
- [5] Carbonari A W, Mestnik-Filho J, Saxena R N and Lalić M V 2004 *Phys. Rev. B* **69** 144425
- [6] Carbonari A W, Mestnik J, Saxena R N, Dogra R and Coaquira J A H 2001 *Hyperfine Interact.* **136/137** 345
- [7] Johansson B and Brooks M S S 1993 *Handbook on the Physics and Chemistry of the Rare Earths* vol 17, ed K A Gschneidner *et al* (Amsterdam: North-Holland) p 149

- [8] Eriksson O, Nordström L, Brooks M S S and Johansson B 1988 *Phys. Rev. Lett.* **60** 2523
- [9] Nordström L, Brooks M S S and Johansson B 1992 *Phys. Rev. B* **46** 3458
- [10] Delin A, Oppeneer P M, Brooks M S S, Kraft T, Wills J M, Johansson B and Eriksson O 1997 *Phys. Rev. B* **55** R10173
- [11] Severin L and Johansson B 1994 *Phys. Rev. B* **50** 17886
- [12] Forker M 1985 *Hyperfine Interact.* **24–26** 907
- [13] Andersen O K 1975 *Phys. Rev. B* **12** 3060
- [14] Singh D J 1994 *Planewaves, Pseudopotential and the LAPW Method* (Dordrecht: Kluwer–Academic)
- [15] Blaha P, Schwarz K, Madsen G K H, Kvasnicka D and Luitz J 2001 *Wien2k; An Augmented Plane Wave + Local Orbitals Program for Calculating Crystal Properties* ed K Schwarz (Technical University of Vienna; ISBN 3-9501031-1-2)
- [16] Perdew J P, Burke K and Ernzerhof M 1996 *Phys. Rev. Lett.* **77** 3865
- [17] Ammarguella C, Escorne M, Auger A, Beaurepaire E, Ravet M F, Krill G, Lapierre F, Haen P and Godrt C 1987 *Phys. Status Solidi* **143** 159
- [18] Liang G and Croft M 1989 *Phys. Rev. B* **40** 361
- [19] Brooks M S S, Eriksson O and Johansson B 1989 *J. Phys.: Condens. Matter* **1** 5861
- [20] Brooks M S S and Kelly P J 1983 *Phys. Rev. Lett.* **51** 1708
- [21] Johansson B, Eriksson O, Nordström L, Severin L and Brooks M S S 1991 *Physica B* **172** 101
- [22] Wulff M, Lander G H, Lebeck B and Delapalme A 1989 *Phys. Rev. B* **39** 4719
- [23] Severin L, Nordström L, Brooks M S S and Johansson B 1991 *Phys. Rev. B* **44** 9392
- [24] Sandratskii L M and Kübler J 1999 *Phys. Rev. B* **60** R6961
- [25] Blügel S, Akai H, Zeller R and Dederichs P H 1987 *Phys. Rev. B* **35** 3271
- [26] Lander G H, Brooks M S S and Johansson B 1991 *Phys. Rev. B* **43** 13672
- [27] Taylor J W, Duffy J A, Bebb A M, Lees M R, Bouchenoire L, Brown S D and Cooper M J 2002 *Phys. Rev. B* **66** 161319(R)
- [28] Lalić M V, Mestnik-Filho J, Carbonari A W, Saxena R N and Haas H 2002 *Phys. Rev. B* **65** 054405